




Novel insight into the etiology of ischemic stroke gained by integrative multiome-wide association study

Junghyun Jung ^{1,*}, Zeyun Lu ², Adam de Smith¹, Nicholas Mancuso ^{1,2,3,*}

¹Center for Genetic Epidemiology, Department of Population and Public Health Sciences, Keck School of Medicine, University of Southern California, 1450 Biggy Street, Los Angeles, CA 90033, United States

²Biostatistics Division, Department of Population and Public Health Sciences, Keck School of Medicine, University of Southern California, 2001 North Soto Street, Los Angeles, CA 90033, United States

³Department of Quantitative and Computational Biology, University of Southern California, 1050 Childs Way, Los Angeles, CA 90089, United States

*Corresponding authors. Center for Genetic Epidemiology, Department of Population and Public Health Sciences, Keck School of Medicine, University of Southern California, 1450 Biggy Street, Los Angeles, CA 90033, United States. E-mail: junghyun.jung@usc.edu and nmancuso@usc.edu

Abstract

Stroke, characterized by sudden neurological deficits, is the second leading cause of death worldwide. Although genome-wide association studies (GWAS) have successfully identified many genomic regions associated with ischemic stroke (IS), the genes underlying risk and their regulatory mechanisms remain elusive. Here, we integrate a large-scale GWAS ($N = 1\,296\,908$) for IS together with molecular QTLs data, including mRNA, splicing, enhancer RNA (eRNA), and protein expression data from up to 50 tissues (total $N = 11\,588$). We identify 136 genes/eRNA/proteins associated with IS risk across 60 independent genomic regions and find IS risk is most enriched for eQTLs in arterial and brain-related tissues. Focusing on IS-relevant tissues, we prioritize 9 genes/proteins using probabilistic fine-mapping TWAS analyses. In addition, we discover that blood cell traits, particularly reticulocyte cells, have shared genetic contributions with IS using TWAS-based pheWAS and genetic correlation analysis. Lastly, we integrate our findings with a large-scale pharmacological database and identify a secondary bile acid, deoxycholic acid, as a potential therapeutic component. Our work highlights IS risk genes/splicing-sites/enhancer activity/proteins with their phenotypic consequences using relevant tissues as well as identify potential therapeutic candidates for IS.

Keywords: ischemic stroke; multiome-wide association study; phenome-wide association study and genetic correlation analysis; drug repositioning

Introduction

Stroke is a complex disease resulting from an interruption of blood flow to the brain [1]. A common type of stroke is ischemic stroke (IS), which is caused by cerebral infarction [2]. Diabetes, obesity, hypertension, and coronary artery disease are well-known risk factors for stroke [3–6], but the pathogenesis of IS is still largely unknown. Although genome-wide association studies (GWAS) have successfully identified genomic regions associated with IS outcomes, the genes underlying IS risk and their regulatory mechanisms remain elusive as the majority of associated variants are non-coding in nature [7, 8].

Recently, the transcriptome-wide association study (TWAS) approach attempts to mitigate this gap in understanding by integrating GWAS associations together with molecular quantitative trait loci (molQTL) data [9, 10]. Previous works have leveraged TWAS to identify candidate susceptibility genes for IS risk, however these analyses have three primary limitations. First, previous analyses were limited to integration of molQTLs measured in whole blood, adipose, and brain tissues [11, 12], which may miss disease mechanisms in less understood or unknown disease-relevant tissues [13–15]. Second, prior works

focused on integration of expression QTL (eQTL) and protein QTL (pQTL) [12, 16], which may miss independent regulatory mechanisms important for IS risk. For example, an essential mechanism of gene regulation and a significant factor in genetic risk of disease is the genetic control of alternative splicing (i.e. sQTLs) [17]. Moreover, recent work demonstrated enhancers undergo activity-dependent transcription, resulting in the production of noncoding enhancer RNAs (eRNAs) which serve as a crucial hallmark of enhancer activation [18, 19]. Third, while the GAGASTROKE prioritized relevant tissues for IS by leveraging eQTL data, it relied on the GTEx v7 study ($N = 388$), [12], which had a smaller sample size than the European GTEx v8 study ($N = 588$). Lastly, the L1000 Connectivity Map (CMap), a public database for large pharmacological datasets, provides extensive gene expression profiles of thousands of compounds in various human cell lines [20]. Recent studies have successfully provided novel therapeutic candidates by utilizing TWAS results with the pharmacological database [21, 22].

Here, we integrate large-scale IS GWAS data ($N = 62\,100$ cases and $1\,234\,808$ controls) with gene expression, alternative splicing, eRNA and protein abundance data ($N = 11\,588$) from 50 different

Received: April 13, 2023. Revised: September 14, 2023. Accepted: October 9, 2023

© The Author(s) 2023. Published by Oxford University Press. All rights reserved. For Permissions, please email: journals.permissions@oup.com

This is an Open Access article distributed under the terms of the Creative Commons Attribution Non-Commercial License (<https://creativecommons.org/licenses/by-nc/4.0/>), which permits non-commercial re-use, distribution, and reproduction in any medium, provided the original work is properly cited. For commercial re-use, please contact journals.permissions@oup.com

tissues to identify IS susceptibility genes, tissues, and drug targets. We identify 136 genes/splicing sites/eRNA/proteins across 54 genomic regions whose genetically predicted activity is associated with IS risk using a multi-tissue mRNA/splicing/eRNA/protein transcriptome-wide association study (TWAS/spTWAS/eTWAS/PWAS). We leverage TWAS results to identify tissues relevant for IS risk and find arterial and brain most enriched for eQTL mediated heritability. Focusing on the IS-relevant tissues, we perform probabilistic fine-mapping analyses of TWAS results to prioritize 9 putative causal genes/proteins. Among them, only 3 genes/proteins (i.e. FOX2, F11, MMP12) were identified in previous GWAS or TWAS studies [7, 12, 16]. In addition, we conduct a TWAS-based pheWAS analysis to understand the phenotypic consequences of identified IS susceptibility genes, and the identified reticulocyte cell traits are significantly correlated with IS. In addition, we discover that reticulocyte traits have shared genetic contributions with IS using TWAS-based pheWAS and genetic correlation analysis. Lastly, to find therapeutic drug candidates for IS risk, we integrate our TWAS findings with 308 872 pairs of compound and compound-perturbed cell-type specific gene expression alterations from the L1000 Connectivity Map. Using this approach, we detect a secondary bile acid, deoxycholic-acid (DCA), as a potential therapeutic component. Overall, our results shed light on underlying molecular mechanisms and tissue contexts that cause ischemic stroke.

Results

Multi-tissue TWAS/spTWAS/eTWAS/PWAS identifies genes/proteins associated with IS risk

To identify susceptibility genes and proteins for IS risk, we conducted a multi-tissue TWAS, spTWAS, and PWAS analysis by integrating large-scale IS GWAS summary statistics ($N = 1\,296\,908$) together with eQTL/spQTL data from GTEx v8 [23] in addition to plasma pQTL data from the INTERVAL [24] and the ARIC [25] studies. Moreover, we performed enhancer TWAS analysis (eTWAS) using brain EeQTL from CMC [19] to investigate the impact of genetic regulation of expressed enhancers on IS risk (see Methods). Focusing on predicted mRNA expression, we tested 309 826 panel-specific expression models across 28 073 genes and identified 268 TWAS associations. Significant associations represented 84 genes across 50 tissues and 45 independent linkage disequilibrium (LD) blocks [26] based on a per-panel Bonferroni correction threshold (Fig. 1A and Supplementary Table S1). Next, to shed light on the role of alternative splicing for IS risk, we performed a multi-tissue splicing transcriptome-wide association study (spTWAS; see Methods). Of the 370 815 panel-specific splicing models with 16 848 tested genes, we identified 498 spTWAS associations. Associations represented 69 unique genes across 48 tissues at 29 genomic regions, the same as TWAS analysis (Fig. 1B and Supplementary Table S2). In addition, we carried out an eTWAS to investigate expressed enhancer effects in two brain tissues using 10 622 tissue-specific eTWAS models with 8397 eRNAs. We identified two enhancers, chr4:186651582:186652095 and chr16:87541308:87541807, in DLPCF and ACC tissues, respectively (Fig. 1C and Supplementary Table S3). Lastly, we focused on the impact of genetically predicted protein abundance by performing a PWAS using 2299 panel-specific protein abundance models with 1556 proteins. We identified 7 PWAS associations across 6 proteins with 6 genomic regions (Fig. 1D and Supplementary Table S4). PWAS results from both pQTL panels showed strong positive correlation ($R = 0.79$; P -value $< 2.2 \times 10^{-16}$; Supplementary Fig. S1), suggesting that the genomic component of

protein abundance is well-captured by fitted models. Comparing the analysis results of TWAS and spTWAS, a total of 21 genes were implicated by both approaches, with ABO and F11 representing the genes or proteins identified by all three approaches (Supplementary Fig. S2A). Among the genomic regions examined, the chr4:186651582:186652095 region was implicated by TWAS/spTWAS/eTWAS/PWAS approaches (Supplementary Fig. S2B). Additionally, the genomic region chr12:110336719:11326351 covers a total of 17 genes or proteins, which is the region with the highest number of genes or proteins. In summary, we identified 60 genomic regions with a total of 136 susceptibility genes, splicing sites, eRNA, and proteins based on multi-tissue TWAS/spTWAS/PWAS approaches. Among the 60 genomic regions we identified, 18 regions overlapped with the GIGASTROKE GWAS result that we used in this study [16].

To provide additional support for genes identified using TWAS, we re-performed analyses using independent approaches and prediction models. First, we compared TWAS and spTWAS results with those computed by S-PrediXcan [27], an independent method to perform a TWAS analysis and fit predictive models. We found S-PrediXcan results were strongly correlated with FUSION-based TWAS ($R = 0.80$; P -value $< 2.2 \times 10^{-16}$) and spTWAS ($R = 0.82$; P -value $< 2.2 \times 10^{-16}$; Supplementary Fig. S3). Second, we carried out a co-localization analysis, which reports the posterior evidence that two phenotypes share a causal variant. Here, we identified 51.49% (138 out of 268) TWAS associations exhibited evidence of co-localization between GWAS signals and eQTLs (Supplementary Table S1). Similarly, among the 498 spTWAS associations, we observed that 271 associations (54.41%) had evidence of co-localization between IS GWAS signal and spQTL association (Supplementary Table S2). We observed that the H_4 posterior probability (PP) of co-localization, correlated with the TWAS ($R = 0.52$; P -value $< 2.2 \times 10^{-16}$) and spTWAS ($R = 0.54$; P -value $< 2.2 \times 10^{-16}$). Moreover, concerning the significant 268 TWAS and 498 spTWAS associations, the respective median PP values for $H_3 + H_4$ are 0.98 and 0.99, respectively. (Supplementary Fig. S4). Repeating this analysis for PWAS signals, we observed ABO, F11, and MMP12 displayed evidence of colocalization between GWAS and pQTL signals (Supplementary Table S4). Despite eTWAS identifying 2 eTWAS signals, we found little support for colocalization between eTWAS and IS GWAS (Supplementary Table S3). The GIGASTROKE consortium recently performed IS TWAS analyses based on GTEx v7 prediction models and identified 17 genes across brain, artery, and heart tissues [16]. We sought to assess the stability of these associations by comparing them with our results which leveraged the larger GTEx v8 and INTERVAL/ARIC cohorts. Among the 17 TWAS genes identified in the previous analyses, we found 7 replicated in our TWAS results (average Bonferroni across tissues, $P < 7.39 \times 10^{-6}$). Similarly, we observed a significant correlation between the TWAS effect sizes in the original GIGASTROKE study with those computed using our prediction models ($R = 0.73$; Supplementary Fig. S5). In summary, our findings support a role for genetically regulated expression, splicing, and proteome levels contributing IS risk.

Relevant tissues for IS risk include brain and arterial tissues

Given the broad number of tissues exhibiting TWAS/spTWAS/PWAS associations, we sought to quantify which tissues are most relevant for IS risk for each molecular context. Specifically, we estimated the proportion of heritability mediated by cis-QTL of gene expression levels (h_{med}^2/h_g^2) and alternative splicing levels

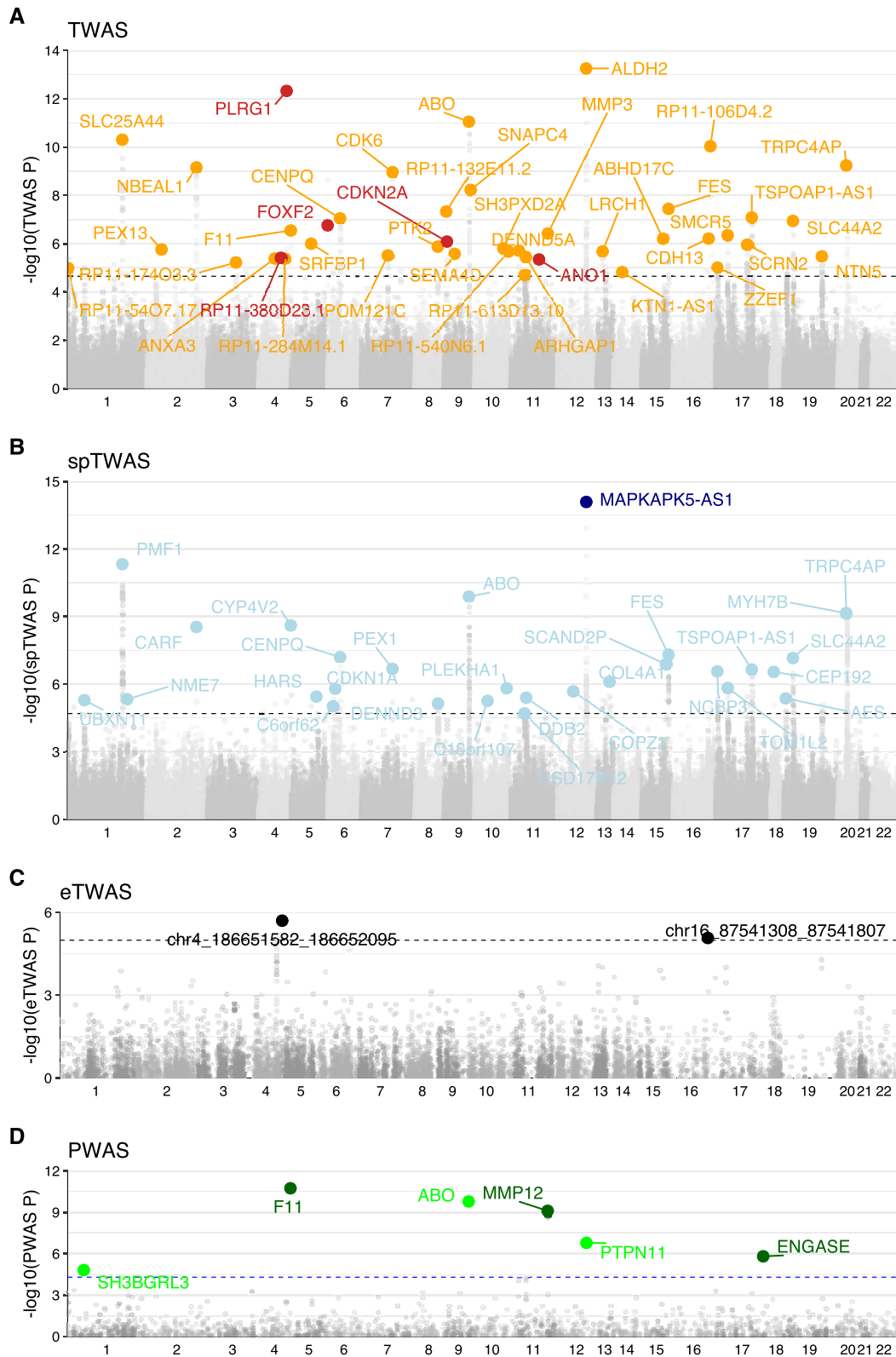


Figure 1. Multi-tissue TWAS/spTWAS/PWAS for IS risk. Manhattan plots of multi-tissue (A) TWAS, (B) spTWAS, (C) eTWAS, and (D) PWAS. Each point corresponds to a P-value (y-axis) of TWAS/spTWAS/eTWAS/PWAS associations across reference panels and chromosomes (x-axis). The most significant associations of TWAS/spTWAS/eTWAS/PWAS genes among reference panels represent different colors, respectively. The dotted lines represent the maximum significant thresholds in this multi-tissue analysis (Supplementary Table S8). The thresholds of TWAS/spTWAS/eTWAS/PWAS indicate 2.23×10^{-5} , 2.00×10^{-5} , 1.02×10^{-5} , and 5.03×10^{-5} , respectively. The putative causal genes (PIP > 0.8) in Table 1 represented gene/proteins of TWAS/spTWAS/PWAS indicating different colors, respectively.

(h_{spmed}^2/h_g^2) using mediated expression score regression (MESC; see Methods) [28]. Using this approach, we identified 3 tissues which exhibited h_{med}^2/h_g^2 estimates greater than 0 at nominal significance (P -value < 0.05). We found “Artery—Aorta” exhibited the greatest h_{med}^2/h_g^2 value ($h_{med}^2/h_g^2 = 0.101$, $s.e. = 0.038$; P -value $= 4.55 \times 10^{-3}$), followed by “Esophagus_Muscularis” ($h_{med}^2/h_g^2 = 0.082$, $s.e. = 0.040$; P -value $= 1.86 \times 10^{-2}$) and “Brain_Amygdala” ($h_{med}^2/h_g^2 = 0.068$, $s.e. = 0.040$; P -value $= 4.55 \times 10^{-2}$) (Fig. 2). The connection between esophagus-muscular tissue and ischemic stroke is not fully understood, but recent evidence suggests that damage to the esophagus-muscular tissue may be a risk factor for ischemic stroke. Previous studies found that people with a history of esophageal disorders, such as gastroesophageal reflux disease (GERD), were more likely to have an ischemic stroke [29, 30]. Our results are supportive of understood IS etiology in which IS occurs due to blood clotting or fatty deposits caused by atherosclerosis that obstruct an artery supplying blood to the brain [31]. Atherosclerosis is commonly thought of as a condition that affects the heart; however, it can also impact arteries located anywhere in the body [32]. In the splicing MESC, “Brain - Nucleus accumbens (basal ganglia)” ($h_{spmed}^2/h_g^2 = 0.085$ and $s.e. = 0.056$) was a high rank in the splicing MESC (Supplementary Fig. S6). Results from expression and splicing MESC showed low correlation across tissues ($R = 0.33$; P -value $= 2.24 \times 10^{-2}$; Supplementary Fig. S7 and Supplementary Table S5). Additionally, we observe a positive correlation between tissue GTEX sample size and the magnitude of expression MESC ($R = 0.35$; P -value $= 0.01$); however, there is no significant relationship between splicing MESC and the sample size ($R = -0.06$; P -value $= 0.67$; Supplementary Fig. S8).

Fine-mapping analysis identifies 9 causal genes/proteins for IS risk

Next, we performed TWAS fine-mapping analysis to identify putative causal genes with multiple signals in the TWAS region prioritizing IS-associated tissues obtained from the MESC analysis [33] (Fig. 2). Among the 84 TWAS significant genes, we identified 5 with posterior inclusion probability (PIP) > 0.8 , which we denote as putative causal genes for IS (Table 1). For example, ANO1 (PIP $= 0.89$; also known as TMEM16A) is suggested to regulate calcium-activated chloride channels and has prior evidence in mouse ischemic stroke models where inhibition of ANO1 expression levels attenuated ischemic brain injury by neurological impairment [34]. We separately performed spTWAS fine-mapping analysis to identify splice variation that may be causally related to IS risk prioritizing brain tissues obtained from splicing MESC analyses. Of the 69 spTWAS significant genes, we identified only MAPKAPK5-AS1 with PIP > 0.8 (Table 1). The mitogen-activated protein kinase (MAPK)-activated protein kinase 5 (APK5), a member of the serine/threonine kinase family, is activated by cellular stress and proinflammatory cytokines [35]. The MAPKAPK5 Antisense RNA 1 (MAPKAPK5-AS1) prevents MAPKAPK5 from being translated into a protein and recent study showed that IS-like pathology was ameliorated by inhibiting the MAPK signaling pathway [36]. Lastly, we performed PWAS fine-mapping to identify protein levels causally relevant to IS risk. Of the 7 PWAS significant associations identified, we found 3 with PIP > 0.8 (Table 1). Of these 3, F11 and MMP12 genes were identified in a previous TWAS of IS risk [12]. Together, we prioritize 9 putative causal genes/proteins based on relevant tissue for IS risk.

IS susceptibility genes correlate with reticulocyte cell traits

To understand the phenotypic consequences of identified IS susceptibility genes, we performed a TWAS-based pheWAS analysis (see Methods). Analogous to the TWAS approach, the TWAS-based pheWAS approach has produced more biologically interpretable results by mapping the genome to the phenome using the transcriptome [37]. We identified 71 traits across a broad range of physical measures (47.9%) and blood cell traits (33.8%) (Supplementary Fig. S9). In the category of physical measures, an average of 25.4% of genes (11.7/46 genes) detected only by spTWAS analysis were enriched, whereas an average of 34.7% of genes (7.3/21 genes) associated with both TWAS and spTWAS were mostly enriched in blood cell traits (Supplementary Table S6). Next, we applied genetic correlation analysis to test whether the PheWAS traits shared genetic contributions with IS at a transcriptome- or proteome-wide level (see Methods). The results show that the well-known risk factors for stroke, such as “Diastolic blood pressure, automated reading (4079_irtnt)”, “Systolic blood pressure, automated reading (4080_irtnt)”, “Non-cancer illness code, self-reported: hypertension (20002_1065)”, “Vascular/heart problems diagnosed by doctor: High blood pressure (6150_4)”, and “Non-cancer illness code, self-reported: high cholesterol (20002_1473)” [4, 39, 39], were significantly correlated with IS in the physical measures and medical conditions categories ($FDR < 0.05$) (Fig. 3 and Supplementary Table S7). Notably, 5 reticulocyte traits, including “Reticulocyte count (30250_irtnt)”, “Reticulocyte percentage (30240_irtnt)”, “High light scatter reticulocyte percentage (30290_irtnt)”, “High light scatter reticulocyte count (30300_irtnt)”, and “Immature reticulocyte fraction (30280_irtnt)”, were significantly positively correlated with IS in TWAS and spTWAS levels in the blood cell traits ($FDR < 0.05$). Reticulocytes are slightly immature red blood cells, and immature reticulocyte fraction levels are associated with acute infection, chronic renal insufficiency, and hematologic diseases [40]. Next, we performed Mendelian randomization analysis to determine the causal relationship between reticulocytes and IS. The MR analysis is analysis with distinct genetic instruments associated with five reticulocyte traits, in addition to genetic instruments associated with IS, respectively. However, we found that there is no causal relationship between IS risk and reticulocyte traits (P -value < 0.01) (Supplementary Fig. S10). Previous studies showed that high reticulocyte count or reticulocytosis are risk factors for stroke in children with sickle cell disease [41–43]. Additionally, we also used LD-score regression (LDSC) to measure shared genetic contributions between traits at the genome-wide level. We found significant correlations between IS and the reticulocyte traits and the well-known risk factors. Collectively, our results show that vascular traits and blood cell traits, especially reticulocyte cells, have shared genetic contributions with IS.

TransPhar analysis identifies secondary bile acids as potential drug candidates for IS

Next, we sought to find potential drug candidates for IS treatment by evaluating an inverse expression relationship with compound-induced gene expression profiles from a large-scale pharmacological database, L1000 CMap [20]. We computed the rank correlations using Spearman’s rank correlation coefficient between the top 10% TWAS genes (or the 134 TWAS/spTWAS/PWAS genes) from each GTEX tissue (a total of 29 GTEX tissues) and each CMAP expression level in the same group of tissues or cell types.

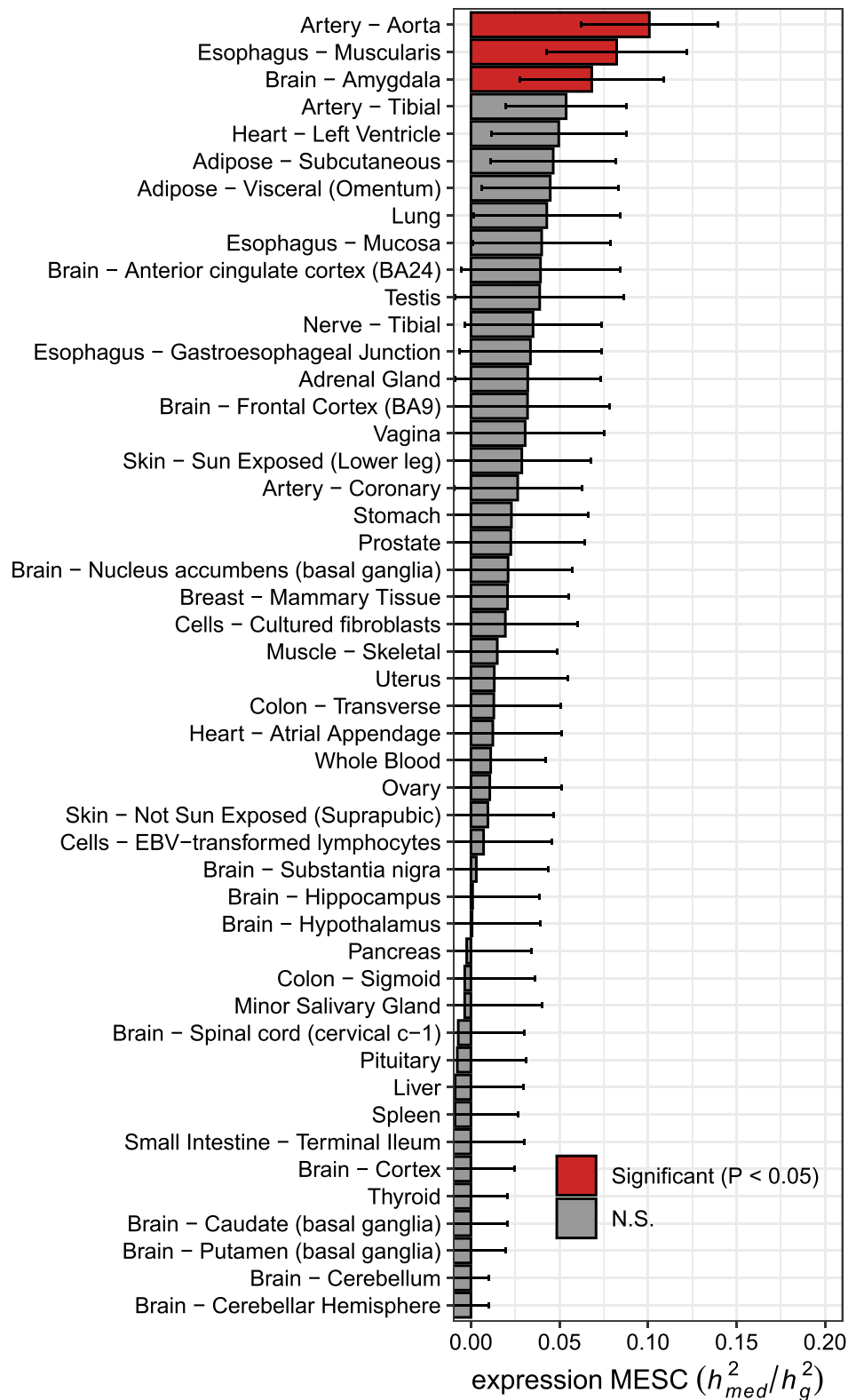


Figure 2. The proportion of heritability mediated by gene expression levels. The bar plots correspond to the estimated expression MESC (h_{med}^2/h_g^2) in each tissue panel in GTEx v8. Each error bar indicates jackknife standard errors.

The top 10% TWAS genes of each tissue contained an average of about 22.26% of the TWAS/spTWAS/PWAS genes (mean 29.82 genes) among the 134 TWAS/spTWAS/PWAS genes or proteins (Supplementary Fig. S11). We obtained 308 872 relationships from all the tissue/cell type-compound pairs corresponding to each

correlation analysis, and the results from the top 10% TWAS genes and the 134 TWAS/spTWAS/PWAS genes were significantly correlated in each tissue (Supplementary Fig. S12). Finally, we found two significant TWAS-compound linkages based on false discovery rate (FDR) correction (Table 2, Supplementary Figs S13

Table 1. Putative causal genes/splicing site/proteins from TWAS/spTWAS/PWAS (PIP > 0.8).

Type	Panel	Tissue	Chr	Symbol	Exon/Intron junction ^a	FUSION TWAS P-value	FOCUS LD block	FOCUS PIP ^b	
								Artery	Brain
TWAS	GTEx	Esophagus Mucosa	4	PLRG1	-	4.69e-13	155 056 126-157 485 097	1	1
TWAS	GTEx	Pituitary	4	RP11-380D23.1	-	3.84e-06	111 256 567-113 870 102	0.999	0.999
TWAS	GTEx	Cells Cultured Fibroblasts	6	FOXF2	-	1.74e-07	73 924-1 452 362	0.995	0.995
TWAS	GTEx	Brain Cortex	9	CDKN2A	-	8.17e-07	20 463 534-22 206 559	-	0.87
TWAS	GTEx	Artery Tibial	11	ANO1	-	4.50e-06	69 516 130-70 926 292	0.891	-
spTWAS	GTEx	Nerve Tibial	12	MAPKAPK5-AS1	112 279 274-112 279 488	8.10e-15	110 336 719-113 263 518	0.965	0.966
PWAS	ARIC	Plasma Protein	4	F11	-	1.82e-11	186 909 090-188 472 981	0.981	-
PWAS	ARIC	Plasma Protein	11	MMP12	-	7.81e-10	101 331 121-103 959 636	0.865	0.865
PWAS	ARIC	Plasma Protein	17	ENGASE	-	1.55e-06	76 263 413-77 298 636	0.945	-

^aAll genomic locations are GRCh37. ^bFOCUS PIP values are obtained by tissue prioritization using "Artery" or "Brain" tissue.

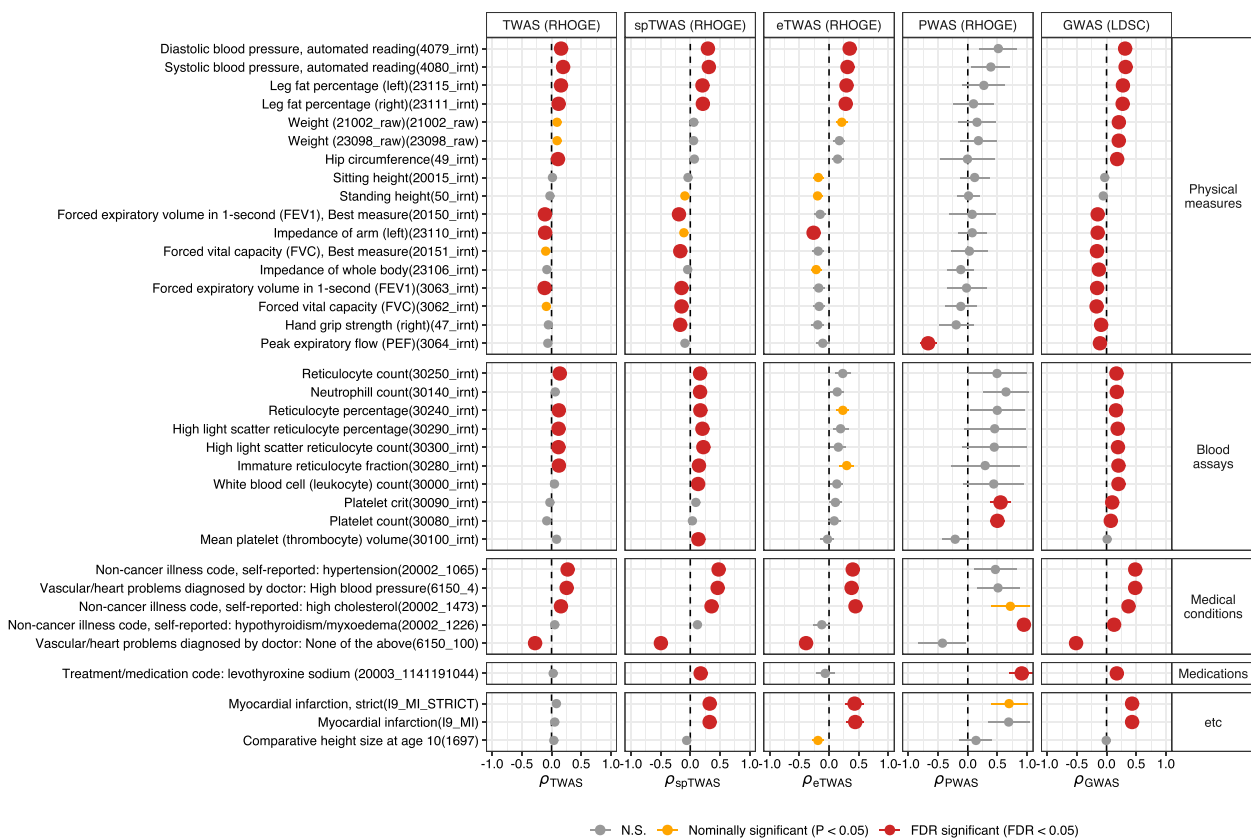


Figure 3. Genetic correlation between IS and UKBB phenotypes. Each point indicates a genetic correlation with TWAS/spTWAS/eTWAS/PWAS standard errors. We use the following abbreviations ρ_{TWAS} , transcriptomic correlation analysis using TWAS; ρ_{spTWAS} , transcriptomic correlation analysis using spTWAS; ρ_{eTWAS} , transcriptomic correlation analysis using eTWAS; ρ_{PWAS} , proteomic correlation analysis using PWAS; ρ_{GWAS} , genomic correlation analysis using GWAS. The figure shows results indicating significance in at least one TWAS/spTWAS/eTWAS/PWAS analysis.

and S14). The two compounds were associated with brain tissue; among them, the mechanism of action has been elucidated for deoxycholic-acid (DCA). The DCA is classified as secondary bile acids, which are produced by gut microbiota [44]. Previous studies showed that other types of secondary bile acids, such as Ursodeoxycholic acid (UDCA) and tauroursodeoxycholic acid (TUDCA), have demonstrated neuroprotective effects in diverse models of neurodegenerative disorders [45–49] as well as stroke [50]. Notably, lower levels of total bile acid excretion is linked to an increased risk of stroke and death [51]. The GIGASTROKE consortium carried out the inverse relationship analysis between

TWAS gene and compound expression levels using GTEx v7 data, but there were no significant results for IS [16]. In summary, our results suggest that a negative correlation between the TWAS genes and compound-induced gene expression levels provides the potential drug candidates for IS.

Discussion

Stroke is the second leading cause of death worldwide, and the main cause of stroke is ischemic stroke (IS) due to cerebral infarction [2]. In this work, we identify 136 susceptibility genes,

Table 2. Potential drug candidates for IS.

Tissue/cell-type categories	GTEX panel (tissue)	CMap L1000 cell line	CMap L1000 library (dose, h)	Mechanism of action	rho (ρ)	P-value	FDR
Brain	Brain - Frontal Cortex BA9	Neural progenitor cells (NPC)	Deoxycholic-acid (DCA) (10 μ M, 24 h)	Fat emulsification	-0.301	8.00e-06	5.46e-02
			BRD-K41878610 (10 μ M, 24 h)	NA	-0.293	1.32e-05	5.46e-02

Rho (ρ) represents Spearman's rank correlation coefficient, and FDR represents the false discovery rate.

splicing sites, eRNA, and proteins spanning 60 genomic regions based on multi-tissue TWAS/spTWAS/PWAS analysis. Among them, 42 genomic regions were not discovered by the original GWAS study. Consequently, we highlight 9 potential causal genes/proteins using probabilistic fine-mapping analysis of the TWAS results with a focus on the IS-relevant tissues, including the aorta artery and brain estimated by a total fraction of disease heritability mediated by gene expression levels. Moreover, we discovered that blood cell traits, particularly reticulocyte cells, have shared genetic contributions with IS. Lastly, we detected 2 potential therapeutic compounds for using inverse expression profiles between TWAS results with compound-induced gene expression profiles from a large-scale pharmacological database.

The genes underlying IS risk and their regulatory mechanisms are still unknown, despite the fact that GWAS have effectively identified numerous genomic regions related to IS, because around 90% of the GWAS loci are located in non-coding regions [7, 8]. However, the TWAS methodology has produced more biologically interpretable results by integrating GWAS results with mQTL data, such as eQTL, spQTL, EnQTL, and pQTL [9, 10, 19]. Consistent with the TWAS approach, the PhenomeXcan has allowed us to identify the mediating role of gene expression in complex traits and convert variant-phenotype associations into gene-phenotype associations by providing biological hypotheses [9, 52, 53]. In recent years, there has been increasing interest in the combination of eQTL and sQTL data to gain a more comprehensive understanding of gene regulation. However, the GTEx project demonstrated that out of the 5385 significant GWAS associations related to 87 complex traits, 43% of the GWAS loci co-localized with cis-eQTL, whereas only 23% of the loci exhibited co-localization with cis-sQTL [23]. Additionally, a previous study revealed that nearly half (52%) of the identified sQTLs also function as eQTLs for the corresponding gene and tissue [54]. These results suggest that the two regulatory mechanisms, eQTL and sQTL, are not consistently interdependent, and the observed low correlation ($R=0.33$) between expression MESC with eQTLs and splicing MESC with sQTLs using sQTLs is not unexpected (Supplementary Figs S7 and S8). The expressed eRNAs have become a hallmark of active enhancers [55]. The effects of disease-associated genetic variants within the enhancer region (i.e. EeQTLs) may offer valuable insights into the regulatory mechanisms of complex diseases. It is important to observe that EeQTLs play a significant role in mediating a considerable portion of heritability associated with neuropsychiatric traits, such as schizophrenia [19], in brain tissue. However, it is noteworthy that the heritability of enhancers (EeQTLs) appears to be lower than that of gene expression (eQTLs) in the CMC panel. The results suggest that the statistical power for detecting associations in eTWAS is considerably reduced in comparison to traditional TWAS approaches. Furthermore, the overall heritability observed in CMC is lower than that observed in the GTEx panel (Supplementary Fig. S15). Additionally, our current study exclusively focused

on conducting eTWAS analysis solely on brain tissues. We do note that exploring the application of eTWAS on arterial tissues, which are relevant to IS, would be an intriguing future study.

A notable finding was the significantly positive correlation between IS risk and reticulocyte traits (Fig. 3). Reticulocytes are slightly immature red blood cells, and higher reticulocyte counts or percentages indicate higher hemolysis, which ultimately results in an increase in the amount of cell-free hemoglobin (CFH) in the blood [56]. The previous studies showed that the hemolysis and the CFH increase inflammation [57] and mediate vascular damage [58]. The findings suggested that a shared causal mechanism influences the high level of reticulocytes with hemolysis and the risk of IS.

After an initial ischemic stroke or transient ischemic attack (TIA), a short episode with temporary blockage of blood flow to the brain, the annual risk of future ischemic stroke is 3% to 5% [59]. The TIA does not leave an impairment, but affected individuals are at increased risk of future ischemic events, especially in the days and weeks immediately after symptoms resolve [60]. The prompt initiation of a coordinated preventive strategy for IS is essential [61].

Recent studies have reported that the probability of success for clinical trials whose therapeutic targets are supported by human genetic information is approximately twice the probability of success for unsupported projects [62, 63]. Taking advantage of the rapid growth of genomics fields, the utilization of human genetics information for new therapeutics has been performed in recent years [21, 22, 64, 65]. Importantly, 66% (33 out of 50) of the FDA-approved new drugs were supported by human genetic information in 2021 [66]. In addition to genetic data, recent gene expression datasets have been leveraged for drug repositioning [67, 68]. In particular, recent studies have investigated the utility of TWAS in drug discovery or repositioning [21, 22]. One primary advantage of the TWAS-based drug repositioning strategy, which integrates large-scale GWAS together with gene expression data, compared with datasets solely comprised of expression is a vastly larger sample size. In general, the sample sizes of GWAS are many orders of magnitude larger (e.g. tens to hundreds of thousands) than those of gene expression datasets (e.g. tens to hundreds). In addition, the TWAS approach enables identifying potential therapeutic compounds that affect multiple tissues (e.g. heart, brain) or cell type-specific contexts by leveraging independent reference eQTL data. On the other hand, the expression data related to the tissue of interest are not easily accessible for many diseases, including IS.

Investigating the causal relationship between the identified repositioning drugs and complex diseases using MR supports the substantiation of the drug repositioning outcomes. Furthermore, by acquiring GWAS data linked to secondary metabolites of the drug candidates, which may directly reflect the actual efficacy of the drug, we can also perform MR analysis to investigate the connection between the secondary metabolites and complex

diseases and traits. This approach is a promising avenue for future research into potential therapeutic compounds.

To shed light on susceptibility genes and mechanisms for IS, we used the recently published GWAS data from the GIGASTROKE consortium. A TWAS analysis was also carried out by the GIGASTROKE group, which discovered 17 genes using prediction models based on GTEx v7 [16]. We found that 7/17 genes replicated with in our TWAS investigation in the brain, artery, and heart tissues with a strong correlation of TWAS effect-sizes ($R=0.73$; [Supplementary Fig. S5](#)). Additionally, we identified 119 genes/proteins and demonstrated some strengths of our study. First, our reference panels for TWAS analysis were significantly larger than the GIGASTROKE study by leveraging GTEx v8 datasets [23], which allowed for more robust analysis and generalization of the findings. Second, our study used a diverse and extensive TWAS analysis, which included a multi-tissue mRNA/splicing/eRNA/protein transcriptome-wide association study (TWAS/spTWAS/eTWAS/PWAS). This diversity provides a broader range of biological mechanisms to understand IS etiology.

We note several limitations with our approach. First, our approach relies on using genetically predicted gene expression levels to identify genes whose expression associates with the genetic component of IS risk, which will require further functional studies for downstream validation. We note however, that our results were robust to choose TWAS approach (i.e. FUSION vs PrediXcan), statistical method (i.e. TWAS vs coloc), and eQTL reference panel (i.e. GTEx v7 vs GTEx v8). Second, we investigated the association between IS risk with diverse molecular contexts focusing on genetically predicted gene expression, protein abundance, splicing variation, and enhancer expression across multiple tissues when available. However, recent works have demonstrated improved association and colocalization power when investigating transcription factor binding, chromatin activity, and chromatin accessibility information [69, 70], which may be potential mediators for IS risk, missed by our work. Despite these limitations, our results provide valuable insights into underlying molecular mechanisms and drug candidates for IS.

In conclusion, we highlight IS risk genes and proteins using the multi-tissue TWAS/spTWAS/eTWAS/PWAS approach. Moreover, we provided potential drug candidates for preventing IS. We believe that these findings could be used as valuable resources for understanding the underlying mechanisms and designing subsequent functional studies for IS treatment.

Materials and methods

Ischemic stroke GWAS summary statistics

IS GWAS summary statistics from GIGASTROKE consortium [16] were downloaded from the GWAS Catalog (GCST90104540) (<https://www.ebi.ac.uk/gwas/studies/GCST90104540>). We restricted summary statistics data to ischemic stroke (AIS) results from 1 296 908 individuals of predominantly European ancestry (62 100 cases and 1 234 808 controls). Next, we filtered summary statistics data to exclude SNPs with minor allele frequency (MAF) < 0.01 or any SNPs with strand-ambiguous variants (i.e. A/T or C/G; or vice-versa) using the focus munge tool [33], resulting in 6 335 571 bi-allelic SNPs for downstream analyses.

Reference functional data for predictive models of eQTL/spQTL/EeQTL/pQTL

To perform TWAS and spTWAS, we generated predictive models of gene and splicing expression using individuals from the Genotype-Tissue Expression Project (GTEx) v8 [23] using a

modified FUSION script (https://github.com/gusevlab/fusion_twass). We downloaded genotype, phenotype, and covariate information from European-American subjects in the GTEx v8 study (48 tissues; $N=588$). We defined the cis-mapping window as ± 500 kb around the transcription start site (TSS) after filtering based on minor allele frequency (MAF) < 0.005 , Hardy-Weinberg Equilibrium (HWE) $< 1 \times 10^{-5}$. We included the reference set of covariates from the GTEx v8 eQTL/spQTL analyses, which included first five genotype principal components (PCs), 15 hidden covariate derived from Probabilistic Estimation of Expression Residuals (PEER) [71] factors, whole genome sequencing (WGS) platform (HiSeq 2000 or HiSeq X), WGS library preparation protocol (PCR-based or PCR-free), and donor gender. We estimated cis-SNP heritability (cis- h^2_g) of each model using REML as implemented in Genome-wide Complex Trait Analysis (GCTA) [72]. We focused on genes and splicing sites with nominally significant estimates of cis- h^2_g (P -value < 0.01), which resulted in 293 295 total tissue-gene pairs from 27 549 unique genes and 371 441 total splicing sites from 16 871 unique genes. To train and generate predictive models, we fitted LASSO [73], Elastic Net [74], and the Sum of Single Effects model (SuSiE) [75]. The best performing model for each gene/tissue (splice-site/tissue) context was selected by calculating cross-validation prediction accuracy, as implemented in the FUSION pipeline. The GTEx v8 weights were publicly available (<http://gusevlab.org/projects/fusion/>).

To perform enhancer TWAS analysis (eTWAS), we downloaded precalculated FUSION weights for enhancer eQTL (EeQTL) data from two brain tissues, the dorsolateral prefrontal cortex (DLPFC) ($N=486$) and the anterior cingulate cortex (ACC) ($N=402$), in CommonMind Consortium (CMC) [19]. Briefly, the LASSO [73], Elastic Net [74] were used to train and generate the eTWAS predictive models for the ACC (4907 predictive models) and DLPFC (5715 predictive models). In addition, we also downloaded fitted prediction models of gene expression in both ACC (8021 predictive models) and DLPFC (8946 predictive models) tissues. For detailed information of the eTWAS and TWAS predicted models, see the previously described ref [19].

To perform a proteome-wide association study (PWAS), we downloaded fitted prediction models of protein abundance trained using individuals from the INTERVAL ($N=3301$) [24] (<https://www.mancusolab.com/pwas>) and Atherosclerosis Risk in Communities (ARIC) [76] (<http://nilanjanchatterjeelab.org/pwas/>) cohorts. In the ARIC cohort, we focused only on the European ancestry dataset ($N=7213$). Briefly, to train and generate the PWAS predictive models using FUSION script, the LASSO [73], Elastic Net [74], and SuSiE [75] were used for the INTERVAL (994 predictive models) and the Elastic Net [74] was used for the ARIC (1305 predictive models). For detailed information of the PWAS predicted models, see the previously described INTERVAL [77] and the ARIC [25].

Transcriptome-wide association study analyses

We performed TWAS, spTWAS, eTWAS, or PWAS analyses using FUSION [9] with the trained GTExv8 [23], CMC [19], or INTERVAL [77] and ARIC [25] models, respectively. European LD reference data from the 1000G project [78] was used for TWAS analysis. We excluded TWAS associations from human leukocyte antigen (HLA) regions due to the complex LD patterns. The significance threshold of TWAS associations was determined using a per-tissue Bonferroni correction (Avg num tests = 6770; [Supplementary Table S8](#)). We then carried out an adaptive permutation test using TWAS test statistics for each tissue panel. For this analysis, 10^6 maximum number of permutations was used, and

the significance threshold was corrected with per-tissue Bonferroni correction. The results of full summary statistics for TWAS, spTWAS, eTWAS, and PWAS were publicly available on GitHub (https://github.com/mancusolab/stroke_twas).

To provide partial support for findings from our FUSION TWAS analyses, we leveraged S-PrediXcan [27] with pre-trained Multi-variate Adaptive Shrinkage in R (MASHR)-based models of PredictDB [52, 79]. In GTEX v8, we tested 648 028 and 1 681 295 models of expression and splicing site, respectively.

Colocalization analysis

We performed colocalization analysis to test whether the same causal variants were shared between stroke GWAS and gene/protein expression levels. We used `coloc` r package [75] together with stroke GWAS summary statistics and marginal molecular QTL (molQTL) results from FUSION prediction models. Consequently, the cis-mapping window, which spans ± 500 kb around the TSS, and the filtering criteria employed in this analysis were consistent with those employed in the TWAS analysis. The evidence of colocalization was defined as $PP_3 + PP_4 \geq 0.8$ and $PP_4/PP_3 \geq 2$ where posterior probability (PP) was obtained from hypothesis H_3 and H_4 . H_3 is the PP of GWAS and eQTL signals are associated with different causal variants, and H_4 is the PP of GWAS and eQTL signals are associated and share a single causal variant.

Mediated expression score regression analyses

To identify tissues relevant for IS risk, we used Mediated Expression Score Regression (MESRC) to estimate the proportion of heritability mediated by assayed gene expression levels (h_{med}^2/h_g^2) [28]. For MESRC expression scores, the eQTL effect sizes using the SuSiE model [75] and expression cis-heritability using REML were imported from FUSION GTEX v8 weights. Only SNPs from the HapMap3 [80] were kept for this research.

Fine-mapping of TWAS associations

To differentiate between causal and tagging associations at TWAS risk regions, we performed probabilistic fine-mapping of TWAS results to prioritize genes using the tool FOCUS [33]. We generated an eQTL/spQTL/pQTL weight database for FOCUS by importing our trained GTEX v8 weights from FUSION. To determine approximately independent genomic regions, we used LD block architecture GRCh19 provided by Berisa and Pickrell [26]. The putative causal genes were defined as $PIP \geq 0.8$.

Phenome-wide association studies and genetic correlation analyses

To understand the phenotypic consequences of identified TWAS/spTWAS/PWAS associations, we performed a phenome-wide association study (pheWAS) for each identified gene using PhenomeXcan [37]. Using the TWAS/spTWAS/PWAS genes, phenotypes from the results of pheWAS analysis were reported based on transcriptome-wide significance (P -value $< 2.25 \times 10^{-6}$). In addition, the pheWAS result was filtered by traits involving at least five TWAS genes.

To determine the genetic relationship between IS and the phenotypes identified from PhenomeXcan, we performed genome-wide genetic correlation analyses using RHOGE [81] with publicly available GWAS summary statistics from the UK Biobank (<http://www.nealelab.is/uk-biobank>). First, TWAS/spTWAS/PWAS analyses were performed using the same FUSION pipeline in the IS analysis. Next, we estimated the genome-wide genetic correlation between the IS and the PhenomeXcan traits derived from TWAS

analysis using LD block architecture GRCh38 (https://github.com/jmacdon/LDblocks_GRCh38) MacDonald *et al.* [82]. In addition, we performed SNP-based genetic correlation analysis using LD Score Regression (LDSC) [83] with the GWAS summary statistics data.

Mendelian randomization analysis

To assess causal effects of reticulocyte traits on IS risk, we performed Mendelian Randomization (MR) analysis. To extract instruments for use in MR from the 5 reticulocyte traits including “Reticulocyte percentage (ukb-d-30240_irnt)”, “Reticulocyte count (ukb-d-30250_irnt)”, “Immature reticulocyte fraction (ukb-d-30280_irnt)”, “High light scatter reticulocyte percentage (ukb-d-30290_irnt)”, and “High light scatter reticulocyte count (ukb-d-30300_irnt)”, We utilized the IEU GWAS database (<https://gwas.mrcieu.ac.uk/>), which provides a vast collection of curated, quality-controlled, and standardized GWAS summary datasets. This resource enables the identification of independent instruments and can be accessed through an API. Next, we employed the `clump_data` command in the TwoSampleMR R package to identify an independent set of variants as genetic instruments using genome-wide significance (P -value $< 5 \times 10^{-8}$) SNPs with LD-pruned (distance threshold = 10 000 kb, $r^2 = 0.001$) [84]. In addition, For the reverse relationship between reticulocyte traits and IS risk, the fine-mapping results of GIGASTROKE [16] were used as instruments. After harmonizing the effect of a SNP on the between IS and reticulocyte traits to the same allele, the MR analysis was conducted using 5 MR method (“MR Egger”, “Weighted median”, “Inverse variance weighted”, “Simple mode”, and “Weighted mode”) [85].

Drug repositioning analysis

To identify potential drug candidates for IS, we used Trans-Phar [21] by comparing the inverse expression profiles between genetically regulated gene expression from TWAS with compound-induced gene expression profiles from a large-scale pharmacological database. Briefly, we obtained differentially expressed genes (DEGs) data from ref. [21] for each compound-induced gene expression data and used 13 tissue/cell-type categories assigned for 29 GTEX tissues and 77 L1000 Connectivity Map (CMap) cell types. Then, we computed the rank correlations using Spearman’s rank correlation coefficient between the top 10% TWAS genes from each GTEX tissue and each CMAP expression level in the same group of tissues or cell types. In addition, we also calculated the Spearman’s rank correlation coefficient using the 134 TWAS/spTWAS/PWAS genes. Finally, a total of 308 872 P -values were collected for each correlation analysis. The significance threshold of the inverse correlation analysis was determined using a per-tissue or/and per-cell type Bonferroni correction (Supplementary Table S9).

Supplementary data

Supplementary data is available at HMG Journal online.

Conflict of interest statement: The authors have no competing interests.

Funding

This work was funded in part by the National Institutes of Health (NIH) under awards R01HG012133 and R01GM140287.

References

- Virani SS, Alonso A, Aparicio HJ. et al. Heart disease and stroke statistics-2021 update: a report from the American Heart Association. *Circulation* 2021;**143**:e254-743.
- Feigin VL, Brainin M, Norrving B. et al. World stroke organization (WSO): global stroke fact sheet 2022. *Int J Stroke* 2022;**17**:18-29.
- Chen R, Ovbiagele B, Feng W. Diabetes and stroke: epidemiology, pathophysiology, pharmaceuticals and outcomes. *Am J Med Sci* 2016;**351**:380-6.
- Wajngarten M, Silva GS. Hypertension and stroke: update on treatment. *Eur Cardiol* 2019;**14**:111-5.
- Horn JW, Feng T, Mørkedal B. et al. Obesity and risk for first ischemic stroke depends on metabolic syndrome: the HUNT study. *Stroke* 2021;**52**:3555-61.
- Amarenco P, Lavallée PC, Labreuche J. et al. Coronary artery disease and risk of major vascular events after cerebral infarction. *Stroke* 2013;**44**:1505-11.
- Malik R, Chauhan G, Traylor M. et al. Multiancestry genome-wide association study of 520,000 subjects identifies 32 loci associated with stroke and stroke subtypes. *Nat Genet* 2018;**50**:524-37.
- Farh KK-H, Marson A, Zhu J. et al. Genetic and epigenetic fine mapping of causal autoimmune disease variants. *Nature* 2015;**518**:337-43.
- Gusev A, Ko A, Shi H. et al. Integrative approaches for large-scale transcriptome-wide association studies. *Nat Genet* 2016;**48**:245-52.
- Mancuso N, Gayther S, Gusev A. et al. Large-scale transcriptome-wide association study identifies new prostate cancer risk regions. *Nat Commun* 2018;**9**:4079.
- Yang J, Yan B, Fan Y. et al. Integrative analysis of transcriptome-wide association study and gene expression profiling identifies candidate genes associated with stroke. *PeerJ* 2019;**7**:e7435.
- Wu B-S, Chen S-F, Huang S-Y. et al. Identifying causal genes for stroke via integrating the proteome and transcriptome from brain and blood. *J Transl Med* 2022;**20**:181.
- Li Y, Kellis M. Joint Bayesian inference of risk variants and tissue-specific epigenomic enrichments across multiple complex human diseases. *Nucleic Acids Res* 2016;**44**:e144.
- Finucane HK, Reshef YA, Anttila V. et al. Heritability enrichment of specifically expressed genes identifies disease-relevant tissues and cell types. *Nat Genet* 2018;**50**:621-9.
- Hao X, Zeng P, Zhang S. et al. Identifying and exploiting trait-relevant tissues with multiple functional annotations in genome-wide association studies. *PLoS Genet* 2018;**14**:e1007186.
- Mishra A, Malik R, Hachiya T. et al. Stroke genetics informs drug discovery and risk prediction across ancestries. *Nature* 2022;**611**:115-23.
- Li YI, van de Geijn B, Raj A. et al. RNA splicing is a primary link between genetic variation and disease. *Science* 2016;**352**:600-4.
- Ding M, Liu Y, Liao X. et al. Enhancer RNAs (eRNAs): New insights into gene transcription and disease treatment. *J Cancer* 2018;**9**:2334-40.
- Dong P, Hoffman GE, Apontes P. et al. Population-level variation in enhancer expression identifies disease mechanisms in the human brain. *Nat Genet* 2022;**54**:1493-503.
- Subramanian A, Narayan R, Corsello SM. et al. A next generation connectivity map: L1000 platform and the first 1,000,000 profiles. *Cell* 2017;**171**:1437-1452.e17.
- Konuma T, Ogawa K, Okada Y. Integration of genetically regulated gene expression and pharmacological library provides therapeutic drug candidates. *Hum Mol Genet* 2021;**30**:294-304.
- So H-C, Chau CK-L, Chiu W-T. et al. Analysis of genome-wide association data highlights candidates for drug repositioning in psychiatry. *Nat Neurosci* 2017;**20**:1342-9.
- GTEX Consortium. The GTEx consortium atlas of genetic regulatory effects across human tissues. *Science* 2020;**369**:1318-30.
- Sun BB, Maranville JC, Peters JE. et al. Genomic atlas of the human plasma proteome. *Nature* 2018;**558**:73-9.
- Zhang J, Dutta D, Köttgen A. et al. Plasma proteome analyses in individuals of European and African ancestry identify cis-pQTLs and models for proteome-wide association studies. *Nat Genet* 2022;**54**:593-602.
- Berisa T, Pickrell JK. Approximately independent linkage disequilibrium blocks in human populations. *Bioinformatics* 2016;**32**:283-5.
- Barbeira AN, Dickinson SP, Bonazzola R. et al. Exploring the phenotypic consequences of tissue specific gene expression variation inferred from GWAS summary statistics. *Nat Commun* 2018;**9**:1825.
- Yao DW, O'Connor LJ, Price AL. et al. Quantifying genetic effects on disease mediated by assayed gene expression levels. *Nat Genet* 2020;**52**:626-33.
- Sheu J-J, Kang J-H, Lou H-Y. et al. Reflux esophagitis and the risk of stroke in young adults: a 1-year population-based follow-up study. *Stroke* 2010;**41**:2033-7.
- Chang C-S, Chen H-J, Liao C-H. Patients with cerebral stroke have an increased risk of gastroesophageal reflux disease: a population-based cohort study. *J Stroke Cerebrovasc Dis* 2018;**27**:1267-74.
- Arboix A. Cardiovascular risk factors for acute stroke: risk profiles in the different subtypes of ischemic stroke. *World J Clin Cases* 2015;**3**:418-29.
- Libby P, Buring JE, Badimon L. et al. Atherosclerosis. *Nat Rev Dis Primers* 2019;**5**:56.
- Mancuso N, Freund MK, Johnson R. et al. Probabilistic fine-mapping of transcriptome-wide association studies. *Nat Genet* 2019;**51**:675-82.
- Liu P-Y, Zhang Z, Liu Y. et al. TMEM16A inhibition preserves blood-brain barrier integrity after ischemic stroke. *Front Cell Neurosci* 2019;**13**. <https://doi.org/10.3389/fncel.2019.00360>.
- New L, Jiang Y, Zhao M. et al. PRAK, a novel protein kinase regulated by the p38 MAP kinase. *EMBO J* 1998;**17**:3372-84.
- Islam MS, Shin H-Y, Yoo Y-J. et al. Olanzapine ameliorates ischemic stroke-like pathology in gerbils and H₂O₂-induced neurotoxicity in SH-SY5Y cells via inhibiting the MAPK signaling pathway. *Antioxidants (Basel)* 2022;**11**. <https://doi.org/10.3390/antiox11091697>.
- Pividori M, Rajagopal PS, Barbeira A. et al. PhenomeXcan: mapping the genome to the phenome through the transcriptome. *Sci Adv* 2020;**6**. <https://doi.org/10.1126/sciadv.aba2083>.
- Prospective Studies Collaboration, Lewington S, Whitlock G. et al. Blood cholesterol and vascular mortality by age, sex, and blood pressure: a meta-analysis of individual data from 61 prospective studies with 55,000 vascular deaths. *Lancet* 2007;**370**:1829-39.
- Hörnsten C, Weidung B, Littbrand H. et al. High blood pressure as a risk factor for incident stroke among very old people: a population-based cohort study. *J Hypertens* 2016;**34**:2059-65.
- Chang CC, Kass L. Clinical significance of immature reticulocyte fraction determined by automated reticulocyte counting. *Am J Clin Pathol* 1997;**108**:69-73.
- Meier ER, Wright EC, Miller JL. Reticulocytosis and anemia are associated with an increased risk of death and stroke in the newborn cohort of the cooperative study of sickle cell disease. *Am J Hematol* 2014;**89**:904-6.

42. Silva CM, Giovani P, Viana MB. High reticulocyte count is an independent risk factor for cerebrovascular disease in children with sickle cell anemia. *Pediatr Blood Cancer* 2011;**56**:116–21.
43. Belisário AR, Sales RR, Toledo NE. et al. Reticulocyte count is the most important predictor of acute cerebral ischemia and high-risk transcranial Doppler in a newborn cohort of 395 children with sickle cell anemia. *Ann Hematol* 2016;**95**:1869–80.
44. Monte MJ, Marin JGG, Antelo A. et al. Bile acids: chemistry, physiology, and pathophysiology. *World J Gastroenterol* 2009;**15**:804–16.
45. Dionísio PA, Amaral JD, Ribeiro MF. et al. Amyloid- β pathology is attenuated by tauroursodeoxycholic acid treatment in APP/PS1 mice after disease onset. *Neurobiol Aging* 2015;**36**:228–40.
46. Lo AC, Callaerts-Vegh Z, Nunes AF. et al. Tauroursodeoxycholic acid (TUDCA) supplementation prevents cognitive impairment and amyloid deposition in APP/PS1 mice. *Neurobiol Dis* 2013;**50**:21–9.
47. Abdelkader NF, Safar MM, Salem HA. Ursodeoxycholic acid ameliorates apoptotic cascade in the rotenone model of Parkinson's disease: modulation of mitochondrial perturbations. *Mol Neurobiol* 2016;**53**:810–7.
48. Rosa AI, Fonseca I, Nunes MJ. et al. Novel insights into the antioxidant role of tauroursodeoxycholic acid in experimental models of Parkinson's disease. *Biochim Biophys Acta Mol basis Dis* 2017;**1863**:2171–81.
49. Keene CD, Rodrigues CMP, Eich T. et al. Tauroursodeoxycholic acid, a bile acid, is neuroprotective in a transgenic animal model of Huntington's disease. *Proc Natl Acad Sci U S A* 2002;**99**:10671–6.
50. Rodrigues CMP, Sola S, Nan Z. et al. Tauroursodeoxycholic acid reduces apoptosis and protects against neurological injury after acute hemorrhagic stroke in rats. *Proc Natl Acad Sci U S A* 2003;**100**:6087–92.
51. Charach G, Karniel E, Novikov I. et al. Reduced bile acid excretion is an independent risk factor for stroke and mortality: a prospective follow-up study. *Atherosclerosis* 2020;**293**:79–85.
52. Gamazon ER, Wheeler HE, Shah KP. et al. A gene-based association method for mapping traits using reference transcriptome data. *Nat Genet* 2015;**47**:1091–8.
53. Zhu Z, Zhang F, Hu H. et al. Integration of summary data from GWAS and eQTL studies predicts complex trait gene targets. *Nat Genet* 2016;**48**:481–7.
54. Garrido-Martín D, Borsari B, Calvo M. et al. Identification and analysis of splicing quantitative trait loci across multiple tissues in the human genome. *Nat Commun* 2021;**12**:727.
55. Sartorelli V, Lauberth SM. Enhancer RNAs are an important regulatory layer of the epigenome. *Nat Struct Mol Biol* 2020;**27**:521–8.
56. Astle WJ, Elding H, Jiang T. et al. The allelic landscape of human blood cell trait variation and links to common complex disease. *Cell* 2016;**167**:1415–1429.e19.
57. Meegan JE, Shaver CM, Putz ND. et al. Cell-free hemoglobin increases inflammation, lung apoptosis, and microvascular permeability in murine polymicrobial sepsis. *PLoS One* 2020;**15**:e0228727.
58. Gladwin MT, Kanas T, Kim-Shapiro DB. Hemolysis and cell-free hemoglobin drive an intrinsic mechanism for human disease. *J Clin Invest* 2012;**122**:1205–8.
59. Amarenco P, Lavallée PC, Labreuche J. et al. One-year risk of stroke after transient ischemic attack or minor stroke. *N Engl J Med* 2016;**374**:1533–42.
60. Giles MF, Rothwell PM. Risk of stroke early after transient ischaemic attack: a systematic review and meta-analysis. *Lancet Neurol* 2007;**6**:1063–72.
61. Rothwell PM, Giles MF, Chandratheva A. et al. Effect of urgent treatment of transient ischaemic attack and minor stroke on early recurrent stroke (EXPRESS study): a prospective population-based sequential comparison. *Lancet* 2007;**370**:1432–42.
62. Nelson MR, Tipney H, Painter JL. et al. The support of human genetic evidence for approved drug indications. *Nat Genet* 2015;**47**:856–60.
63. King EA, Wade Davis J, Degner JF. Are drug targets with genetic support twice as likely to be approved? Revised estimates of the impact of genetic support for drug mechanisms on the probability of drug approval. *PLoS Genet* 2019;**15**:e1008489.
64. Okada Y, Wu D, Trynka G. et al. Genetics of rheumatoid arthritis contributes to biology and drug discovery. *Nature* 2014;**506**:376–81.
65. Fang H, ULTRA-DD Consortium, De Wolf H. et al. A genetics-led approach defines the drug target landscape of 30 immune-related traits. *Nat Genet* 2019;**51**:1082–91.
66. Ochoa D, Karim M, Ghossaini M. et al. Human genetics evidence supports two-thirds of the 2021 FDA-approved drugs. *Nat Rev Drug Discov* 2022;**21**:551.
67. Lamb J, Crawford ED, Peck D. et al. The connectivity map: using gene-expression signatures to connect small molecules, genes, and disease. *Science* 2006;**313**:1929–35.
68. Iorio F, Bosotti R, Scacheri E. et al. Discovery of drug mode of action and drug repositioning from transcriptional responses. *Proc Natl Acad Sci U S A* 2010;**107**:14621–6.
69. Grishin D, Gusev A. Allelic imbalance of chromatin accessibility in cancer identifies candidate causal risk variants and their mechanisms. *Nat Genet* 2022;**54**:837–49.
70. Baca SC, Singler C, Zacharia S. et al. Genetic determinants of chromatin reveal prostate cancer risk mediated by context-dependent gene regulation. *Nat Genet* 2022;**54**:1364–75.
71. Stegle O, Parts L, Durbin R. et al. A Bayesian framework to account for complex non-genetic factors in gene expression levels greatly increases power in eQTL studies. *PLoS Comput Biol* 2010;**6**:e1000770.
72. Yang J, Lee SH, Goddard ME. et al. GCTA: a tool for genome-wide complex trait analysis. *Am J Hum Genet* 2011;**88**:76–82.
73. Santosa F, Symes WW. Linear inversion of band-limited reflection seismograms. *SIAM J Sci Stat Comput* 1986;**7**:1307–30.
74. Zou H, Hastie T. Regularization and variable selection via the elastic net. *J R Stat Soc B* 2005;**67**:301–20.
75. Wang G, Sarkar A, Carbonetto P. et al. A simple new approach to variable selection in regression, with application to genetic fine mapping. *J R Stat Soc B* 2020;**82**:1273–300.
76. The Aric Investigators. The atherosclerosis risk in community (ARIC) study: design and objectives. *Am J Epidemiol* 1989;**129**:687–702.
77. Pathak GA, Singh K, Miller-Fleming TW. et al. Integrative genomic analyses identify susceptibility genes underlying COVID-19 hospitalization. *Nat Commun* 2021;**12**:4569.
78. 1000 Genomes Project Consortium, Auton A, Brooks LD. et al. A global reference for human genetic variation. *Nature* 2015;**526**:68–74.
79. Barbeira AN, Bonazzola R, Gamazon ER. et al. Exploiting the GTEx resources to decipher the mechanisms at GWAS loci. *Genome Biol* 2021;**22**:49.
80. International HapMap Consortium. The international HapMap project. *Nature* 2003;**426**:789–96.
81. Mancuso N, Shi H, Goddard P. et al. Integrating gene expression with summary association statistics to identify genes associated with 30 complex traits. *Am J Hum Genet* 2017;**100**:473–87.

82. MacDonald JW, Harrison T, Bammler TK. *et al.* An updated map of GRCh38 linkage disequilibrium blocks based on European ancestry data. *bioRxiv*. 2022; p. 2022.03.04.483057. [https://doi:10.1101/2022.03.04.483057](https://doi.org/10.1101/2022.03.04.483057).
83. Bulik-Sullivan BK, Loh P-R, Finucane HK. *et al.* LD score regression distinguishes confounding from polygenicity in genome-wide association studies. *Nat Genet* 2015;**47**:291–5.
84. Hemani G, Zheng J, Elsworth B. *et al.* The MR-base platform supports systematic causal inference across the human phenome. *elife* 2018;**7**. [https://doi:10.7554/elife.34408](https://doi.org/10.7554/elife.34408).
85. Bowden J, Davey Smith G, Burgess S. Mendelian randomization with invalid instruments: effect estimation and bias detection through Egger regression. *Int J Epidemiol* 2015;**44**: 512–25.